17th World Conference on Earthquake Engineering, 17WCEE
Sendai, Japan - September 27th to October 2nd, 2021

NUMERICAL MODELLING OF THE SEISMIC PERFORMANCE OF CONTROLLED ROCKING MASONRY WALLS WITHOUT POST-TENSIONING

A. Yassin[(1)], M. Ezzeldin[(2)], L. Wiebe[(3)]

[(1)] *Ph.D. Candidate, Department of Civil Engineering, McMaster University, yassia1@mcmaster.ca*
[(2)] *Assistant Professor, Department of Civil Engineering, McMaster University, ezzeldms@mcmaster.ca*
[(3)] *Associate Professor, Department of Civil Engineering, McMaster University, wiebel@mcmaster.ca*

Abstract

Controlled rocking walls are considered an excellent alternative seismic force resisting system for modern resilient cities. This is because of their ability to self-center following seismic events with minimal residual drifts compared to those of conventional walls (i.e. with fixed base). This significantly reduces costs due to service shutdown for structural repairs/replacement. In general, controlled rocking walls depend on unbonded post-tensioning tendons to re-center the wall after loading, thus minimizing or eliminating residual drifts. However, adding post-tensioned tendons in masonry walls create challenges during construction, and prestressing losses are relatively large compared to those in post-tensioned concrete walls. For these reasons, it was desired to investigate an alternative source of self-centering for controlled rocking masonry walls (CRMWs). Recent experimental studies conducted by the authors demonstrated the performance of a new system that relies solely on gravity loads to provide self-centering behavior, while also using supplemental energy dissipation. These walls are termed energy dissipation-controlled rocking masonry walls (ED-CRMWs), and were tested under quasi-static fully-reversed cyclic loading up to failure. The focus of this paper is on a numerical model using OpenSees, based on a multi-spring modelling approach, that simulates the seismic performance of such ED-CRMWs. The model is validated against the experimental results of three ED-CRMWs, which include different confining techniques at the wall compression toes and different energy dissipation locations. The validation results explore the ability of the model to capture the most relevant characteristics of the walls behavior such as load displacement response, lateral load capacity, yield and ultimate displacements, displacement ductility, hysteretic shape and pinching behavior, effective stiffness and energy dissipation at different drift levels for the three specimens.

Keywords: Self-centering; Controlled rocking masonry wall; Reinforced masonry; Energy dissipation; Numerical model

1. Introduction

Conventional fixed-base walls are characterized by significant damage during a design level earthquake, due to extensive yielding associated with large residual lateral displacements and wide residual cracks. Accordingly, prestressed controlled rocking wall systems have received attention through the Precast Seismic Structural Systems (PRESSS) project [1] as an effective seismic force resisting system. The system mainly relies on vertical unbonded post-tensioning, which forces the wall to self-center and reduces the damage due to tension cracks. The PRESSS test results demonstrated that the damage was localized at the wall crushing toes with a single crack at the wall-foundation rocking interface. In addition, the wall response was mainly governed by the rocking deformation while the flexural and shear deformations were minimal [2]. A main advantage of controlled rocking shear walls is that they had almost no permanent drifts at the end of the experimental tests. This behavior is known as self-centering. These promising results led several researchers to perform further investigations in an effort to enhance the seismic performance of controlled rocking concrete [3, 4] and masonry [5-8] shear walls.

The rocking mechanism starts when a lateral load causes the base overturning moment to exceed the wall decompression moment capacity. At that stage, the wall uplifts from the foundation and a single horizontal crack at the wall-foundation interface is formed, as shown in Fig.1. This leads to a reduction in the wall lateral stiffness through an elastic gap opening mechanism, called a rocking mechanism. Such a mechanism replaces the typical yielding of the main reinforcement that occurs in a conventional shear wall (i.e. fixed base wall), and it is controlled by the unbonded post-tensioning steel, which restores the wall system to its vertical alignment. This self-centering ability reduces permanent deformations after a seismic event and therefore, a post-tensioned controlled rocking wall, without damage or a supplemental energy dissipation device, is essentially a nonlinear elastic system. Such a system is favorable for resilient cities, where the costs associated with service shutdown for structural repairs or replacement are minimized. Based on the above, this system is particularly appropriate for structures designed for the immediate occupancy performance level [9].

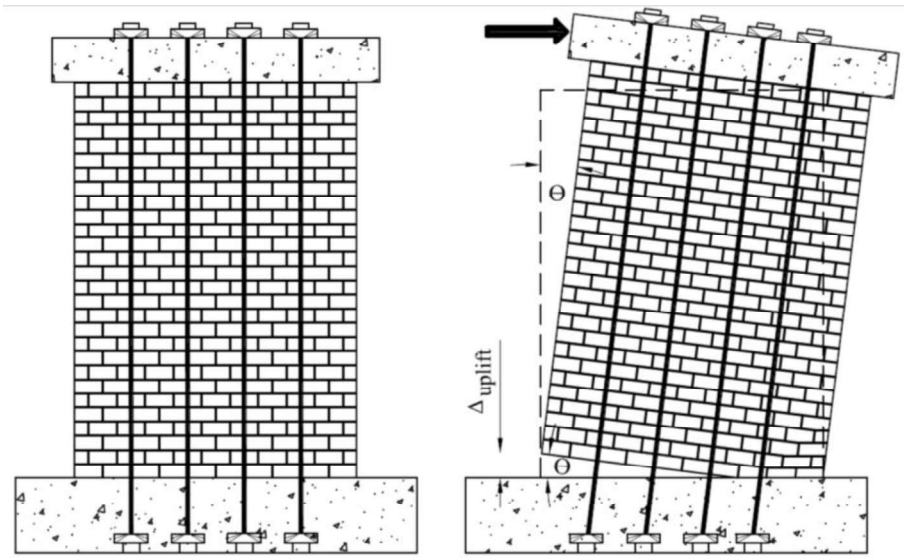

Fig. 1 – Masonry wall rocking mechanism

There are several challenges associated with the use of post-tensioning tendons in masonry construction practice, including tendon losses and other difficulties related to inspections following seismic

events. As such, experimental studies have been performed to explore alternatives to control and self-center rocking masonry walls. Recently, Yassin et al. [10] conducted an experimental investigation on a rocking masonry wall system that relies on gravity loads to self-center the wall, along with an energy dissipation source to control the response by increasing the wall system damping. The experimental results showed that the proposed system, namely, energy dissipation-controlled rocking masonry walls (ED-CRMWs), can self-center the wall with minimum residual drifts and also localize the damage at the crushing toes only, similar to controlled rocking masonry walls with unbonded post-tensioning tendons (PT-CRMWs).

In this respect, the current study develops and validates a numerical model that simulates the seismic response of ED-CRMWs. Specifically, a simplified multi-spring numerical model using OpenSees [11] is developed and validated using three ED-CRMWs that were tested under displacement-controlled cyclic loading. The validation results of the developed model are presented in terms of force-displacement response, lateral load capacity, yield and ultimate displacements, displacement ductility, hysteretic shape and pinching behavior, effective stiffness, and energy dissipation at different drift levels.

2. Experimental Data

The numerical model developed in the current study was validated against the experimental results of three half-scale ED-CRMWs that were tested by Yassin et al. [10]. All three walls were tested under quasi-static reversed cyclic loading with an observed rocking response. Each test was terminated when the wall reached 50% strength degradation or the maximum stroke of the hydraulic actuator was reached. As shown in Fig. 2, the test matrix included an unconfined wall (W1), a confined wall with boundary elements and closed stirrups (W2), and a confined wall with Priestley plates [12] (W3) with energy dissipation close to wall centerline. All these walls were fully grouted and unbonded M10 steel bars were installed internally across the wall-foundation interface as a source of energy dissipation. These bars had an unbonded length of 900 mm to achieve safely the design drift (0.35%) at the design level earthquake without fracture. As shown in Fig. 2, the energy dissipation bar was located at 250 mm from the wall ends for wall W1 and W2, to protect the bar from the crushing zone, hence avoiding premature buckling initiation of the unbonded energy dissipation bar. For W3, the energy dissipation bars were located at 140 mm from wall centerline. The three half-scale walls had the same length (1895 mm), thickness (90 mm) and height (2660 mm), representing two-storey walls. All walls were subjected to an axial load of 200 kN (6.5%$A_g f_m^{/}$) to represent the gravity loads from floors. The closed stirrups used in W2 were located in every other course, while the confining plates (Priestley plates) used in wall W3 were located inside the bed joint of every course within the first five courses near the base. Table 1 presents the complete test matrix, while the wall cross-section details are shown in Fig. 2.

Table 1 – Wall dimensions and properties for model validation

Specimen	Wall Type	Wall Dimension	Vertical Reinforcement	Horizontal Reinforcement	Confinement
W1	Rectangular	1895 mm x 2660 mm x 90 mm	6D7 + 2M10	D4 every other course	N.A.
W2	End-Boundary		4D7+ 2M10 @Web 8D7 @ Ends		D4 closed ties every other course
W3	Rectangular		6D7 + 2M10		Confining plates every course within the first five courses near the base

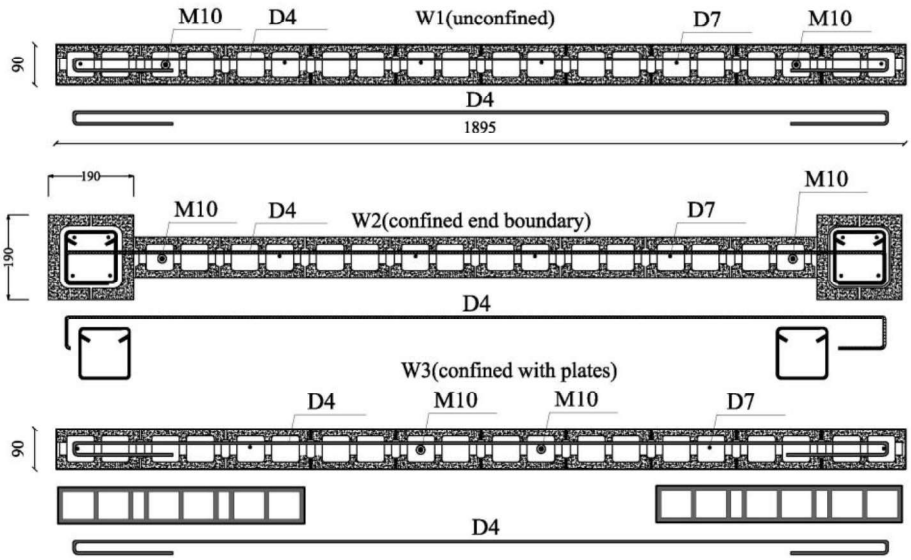

Fig. 2 – Cross sections of tested walls used for model validation (all dimensions are in mm)

3. Model Description

In the current study, OpenSees [11] is used to create macro models to simulate the non-linear response of ED-CRMWs under cycling loading. Building on the model developed by Yassin et al. [8], Fig. 3 shows a schematic diagram of the wall model, which consists of three main elements: 1) a bed of spring elements to represent the wall-foundation rocking interface; 2) truss elements to represent the energy dissipation bars; and 3) inelastic force-based beam-column elements to represent the wall panel.

In this model, the multi-spring analogy is adopted to capture the stresses at the wall-foundation interface. All springs are defined by zero-length elements with a nonlinear constitutive material model to represent the masonry nonlinear behavior. To simulate the wall rocking mechanism and the corresponding uplift, the springs at the wall base are defined by a zero-tensile strength material model. This material model (i.e. Concrete01 in OpenSees) exhibits stiffness degradation upon unloading or reloading and is defined by strains at maximum strength and at crushing. Thus, the descending post peak slope can be controlled to account for any confinement effect. Moreover, during the cyclic loading, the springs experience compression and elongation deformations, which can cause numerical convergence problems. Therefore, the use of the Concrete01 material model for the springs not only yields a smooth transition from compression to tension with no tensile strength during rocking, but also overcomes the numerical convergence issues when other concrete material models are used. To minimize such convergence problems, a spacing of 10 mm between springs is always used in the model [13]. The vertical displacement of the nonlinear zero-length spring elements, corresponding to the strain at the maximum compressive stress in masonry, ε_m, is assumed to be ε_m multiplied by the expected height of the equivalent plastic deformations. As will be shown in the numerical results, the wall response can be well captured if the plastic hinge length, representing the height of equivalent plastic deformations, is reasonably estimated. This approach has previously been validated against experimental results for PT walls by Yassin et al. [8].

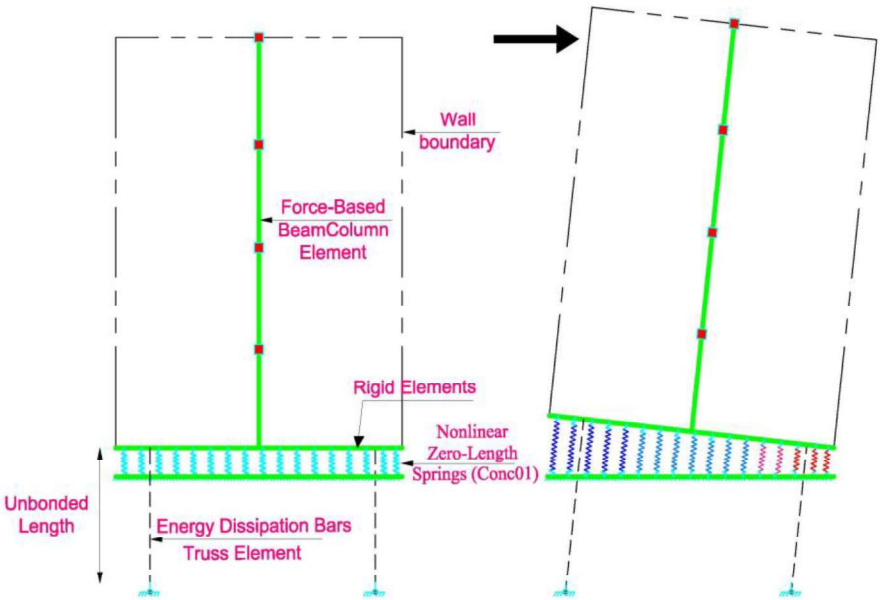

Fig. 3 – Schematic diagram of the developed model

The energy dissipation bars were modeled using the Hysteretic-Material model available in OpenSees. This model captures the buckling/fracture of the bars using PinchX and PinchY values of 0.5. The model was defined using three points in the tension and compression stress-strain curves that corresponds to: 1) the yield strength, f_y, of 450 MPa and the yield strain, ε_y, of 0.0025; 2) one point at the end of the yield plateau (450MPa, 0.005 mm/mm); and 3) the ultimate strength, f_u, of 650 MPa and the ultimate strain, ε_u, of 0.08. These values were taked from uniaxial tension testing of the bars, except that the ultimate strain, ε_u, taken as a reduced value to consider the low cycle fatigue.

The wall panel was modeled using inelastic force-based beam-column elements to capture any inelastic actions throughout wall height from higher mode effects when dynamic loads are applied [8]. However, under static cyclic loading, the use of elastic or inelastic elements yields identical responses. This finding agrees with previous experimental and analytical studies [14, 6], which reported that the behavior of unbonded post-tensioned concrete or masonry walls was elastic at a short distance above the single horizontal crack located at the wall rocking base.

4. Model Validation

The three tested walls (W1, W2 and W3) are used to verify the effectiveness of the developed numerical model. The model is evaluated based on the ability to simulate the experimental results in terms of the most relevant characteristics of the wall behavior such as force-displacement response, lateral load capacity, yield and ultimate displacements, displacement ductility, hysteretic shape and pinching behavior, effective stiffness and energy dissipation at different drift levels. The following subsections quantify the validation of these parameters.

4.1 Overall Force-Displacement Response

As shown in Fig. 4, for all three walls, there is good agreement between the experimental and numerical hysteresis loops. The model is able to simulate the experimental results such as the initial stiffness, peak load, stiffness degradation, strength deterioration, hysteretic loop shape and size at different drift levels. Regarding W2, the sudden strength degradation was due to energy dissipation bar fracture, and this behavior

is captured accurately by the model. In addition, the hysteretic shape of W3 compared to W1 is relatively pinched due to the energy dissipation bar location, which is also captured by the numerical model.

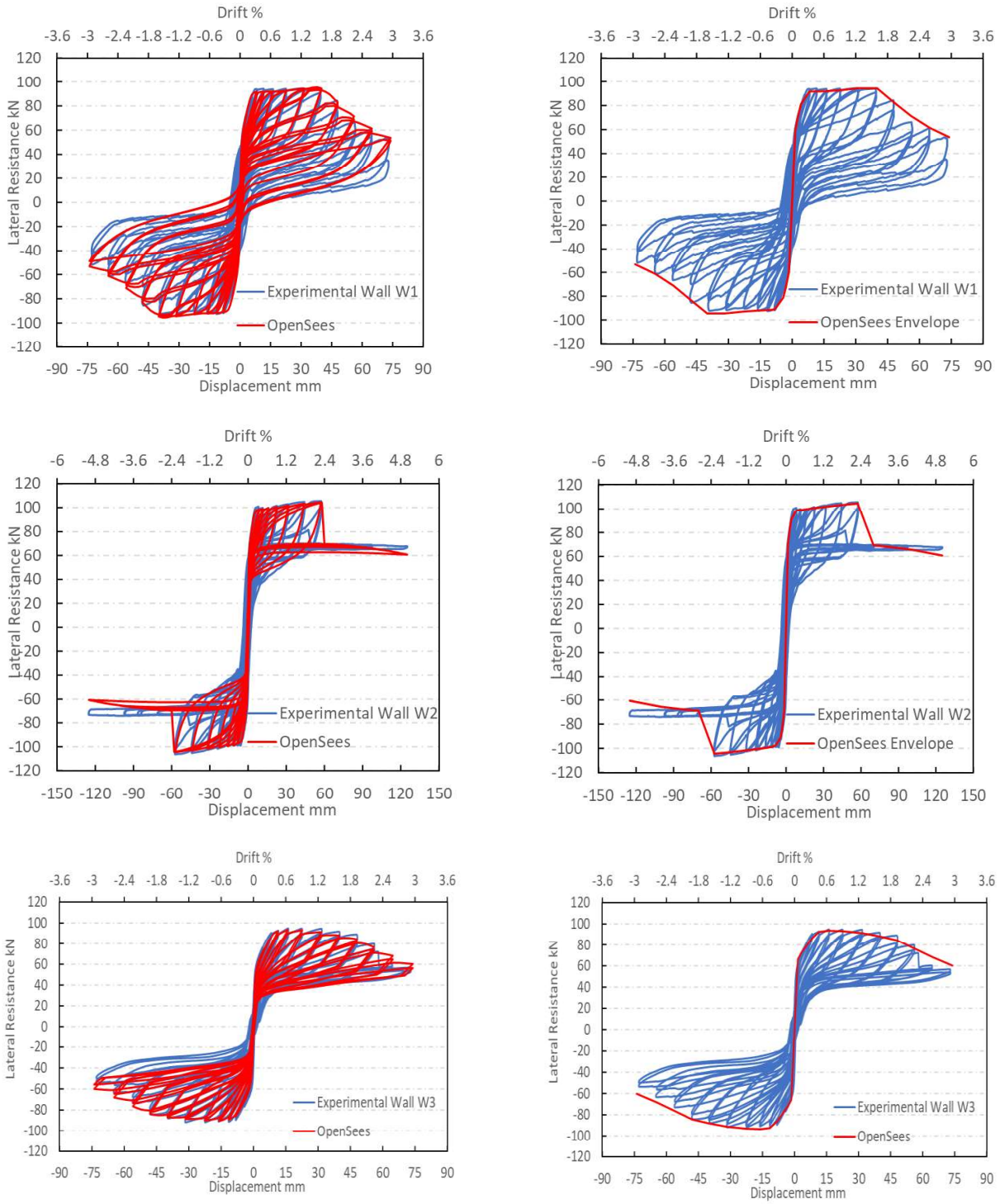

Fig. 4 – Experimental and numerical cyclic response

4.2 Lateral Load Capacity

The numerical and experimental decompression strength, Q_o, yield strength, Q_y, and ultimate flexural strength, Q_u, of all walls are presented in Table 2. The decompression strength, Q_o, is the wall lateral resistance when the wall is about to uplift, and it corresponds to the point at which a sudden change in wall stiffness is observed in the early drift stages before energy dissipation bars yielding. The yield strength, Q_y, is the wall lateral resistance at onset of yielding of the energy dissipation bar. As shown in Table 2, for all walls, the maximum error in decompression strength, Q_o, is 10%, yield strength, Q_y, is 5% and ultimate flexural strength, Q_u, is 2%.

Table 2 – Lateral load capacity comparison

Specimen	Decompression Strength Q_o (kN)			Yield Strength Q_y (kN)			Ultimate Strength Q_u (kN)		
	Numerical	Experimental	Ratio	Numerical	Experimental	Ratio	Numerical	Experimental	Ratio
W1	59.5	55.4	1.07	90.5	92.0	0.98	94.3	94.0	1.00
W2	69.0	63.0	1.09	98.5	100.1	0.98	104.5	105.0	0.99
W3	64.4	58.4	1.10	86.4	90.3	0.95	93.6	94.8	0.98

4.3 Yield and Ultimate Displacements

The numerical and experimental decompression displacement, Δ_o, yield displacement, Δ_y, and ultimate displacement, Δ_u, of all walls are listed in Table 3. As shown in Table 3, for all walls, the maximum errors in decompression displacement, Δ_o, yield displacement, Δ_y, and ultimate displacement, Δ_u, are 10%, 3% and 2%, respectively.

Table 3 – Wall displacements comparison

Specimen	Decompression Displacement Δ_o (mm)			Yield Displacement Δ_y (mm)			Ultimate Displacement Δ_u (mm)		
	Numerical	Experimental	Ratio	Numerical	Experimental	Ratio	Numerical	Experimental	Ratio
W1	1.9	2.1	0.90	4.2	4.3	0.97	40.0	40.0	1.00
W2	1.9	2.0	0.95	4.2	4.1	1.02	57.3	57.3	1.00
W3	1.9	2.1	0.90	8.2	8.3	0.98	16.0	16.2	0.98

4.4 Displacement Ductility

The displacement ductility, μ, is used to evaluate and compare the post-peak behavior of the numerical and the experimental ED-CRMWs. The displacement ductility, $\mu_{0.8u}$, is considered based on 20% strength degradation and defined as the ratio between the displacement corresponding to 20% reduction in peak strength and the displacement corresponding to the onset of energy dissipation bar yielding without any idealization to the load-displacement relationship. As shown in Table 4, the maximum error in the displacement ductility, $\mu_{0.8u}$, is 4% for all three walls.

Table 4 – Displacement ductility comparison

Specimen	Ultimate Displacement at 20% Degradation $\Delta_{0.8u}$ (mm)			Displacement Ductility $\mu_{0.8u}$		
	Numerical	Experimental	Ratio	Numerical	Experimental	Ratio
W1	49.0	48.0	1.02	11.6	11.2	1.04
W2	59.0	59.0	1.00	14.0	14.4	0.97
W3	57.0	56.0	1.01	6.9	6.7	1.02

4.5 Hysteretic Behavior

Fig. 5 compares the individual experimental and numerical hysteresis loops for the three walls at the same drift levels of 1.60% and 2.30% to show the model's accuracy in capturing the hysteretic behavior at peak and post-peak stages. The figure shows that the model can capture the influence of the energy dissipation device on the wall response, where a significant increase in the loop size is observed in all walls after 0.2% drift, as the unbonded steel bars yielded around this drift level. The residual drift for W1 and W2 was underestimated in the 1.60% drift cycle, while better representation of self-centering happens in the 2.30% drift cycle. On the other hand, W3 was accurately represented in both drift cycles, given that the 1.5mm sliding is omitted. The effect of energy dissipation bar buckling in reducing the hysteretic loop size is clearly observed in W2 in the post-peak cycle (2.30% drift), by which no work is exerted by the buckled bar located in the uplifting side of the wall until the buckled bar is straightened (i.e at approximately 1.0% drift) then it starts to carry tension and elongates. Hence, all the strength before this point is coming from the axial load contribution only. The model was able to capture this behavior to a good extent, where Hysteretic Material model was used specifically to model the damage due to buckling. Overall, the individual loops show that the model can simulate and predict the main characteristics of the hysteretic loops such as the loading and unloading stiffness, strength, loop shape and size, as well as the pinching behavior.

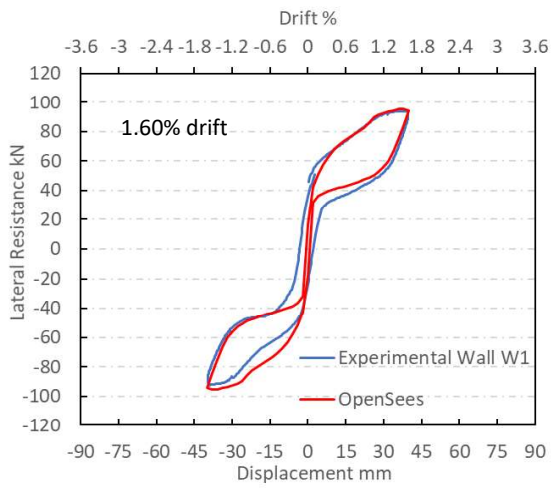

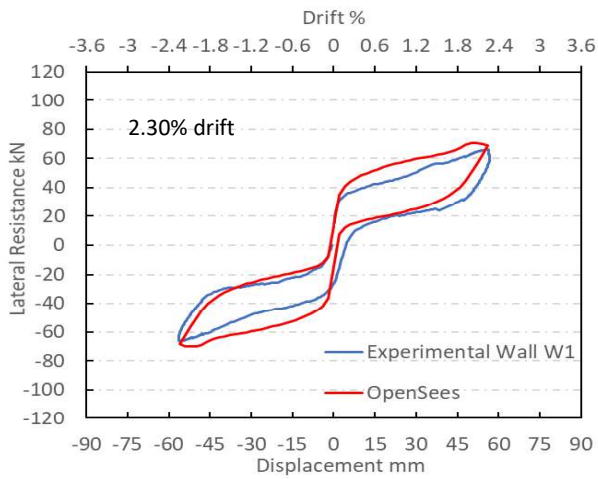

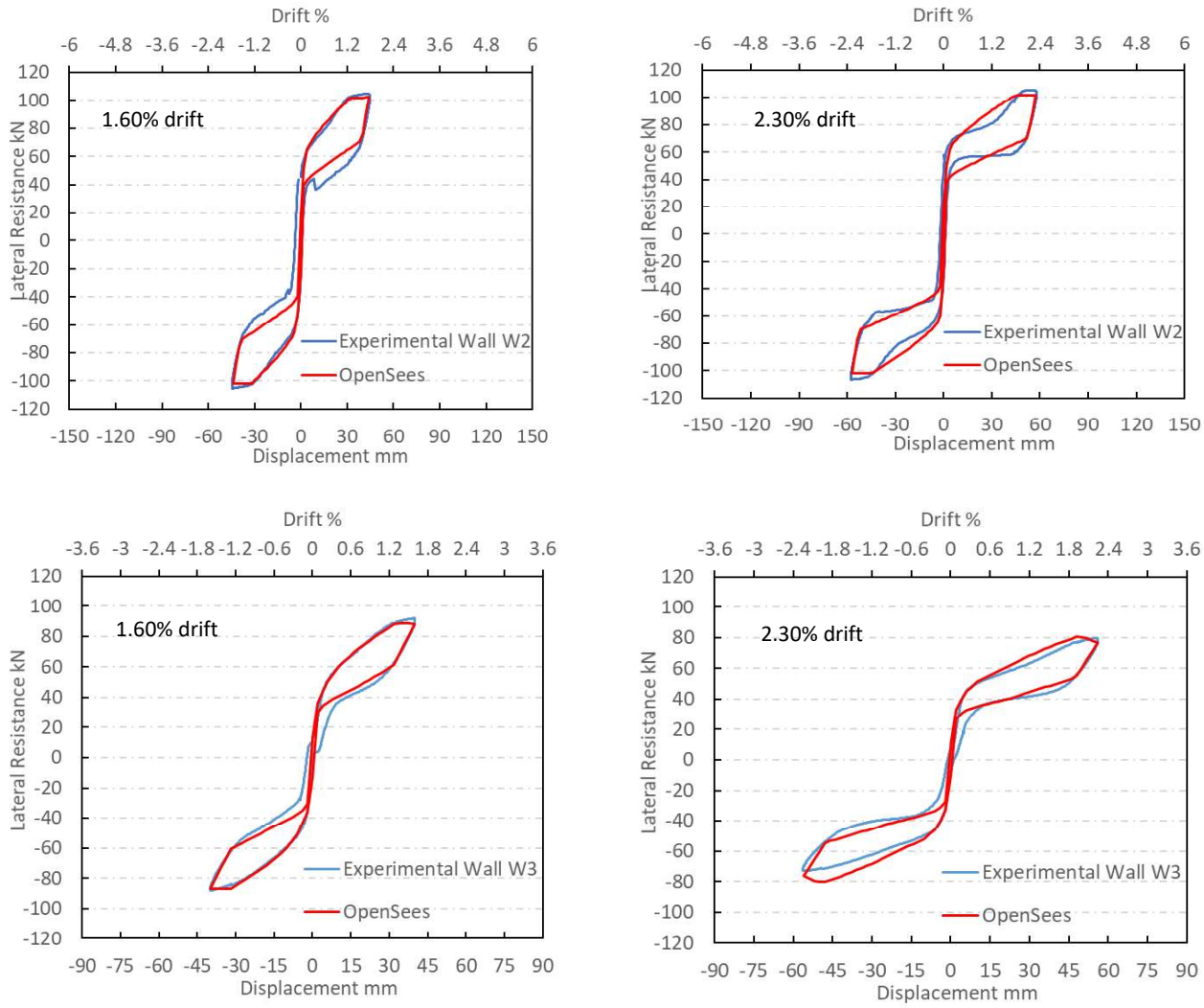

Fig. 5 – Hysteresis loops for walls W1, W2 and W3 at different drift levels

4.6 Effective Stiffness and Energy Dissipation

The effective stiffness, K_{eff}, was calculated according to ASCE 41-17 [15]. Fig. 6 shows how the secant stiffness in each cycle reduces with increasing drift due to gap opening and ED yielding. The numerical model represents the effective stiffness with a high level of accuracy.

The energy dissipation, E_d, is also considered as an important aspect in seismic design because it reduces the amplitude of the seismic response. The energy dissipation is presented here as suggested by Hose and Seible [16], where energy dissipation is calculated by the enclosed area under the force-displacement curve. Fig. 6 shows that the energy dissipated at small drifts before significant yielding is low and increasing gradually due to reaching high values of strains greater than yielding strain of energy dissipation bars (up to 15 ε_y) at higher displacement level. Afterwards, the energy dissipation bars fractured (in case of wall W2) at high drift, leading to a decrease in dissipated energy. The figure shows that the numerical results match the experimental behavior with a sufficient degree of accuracy, where the maximum error in the cumulative energy dissipation is 15%, 19% and 16% for walls W1, W2 and W3, respectively. The value of effective stiffness, K_{eff}, and energy dissipated, E_d, was then used to calculate the equivalent viscous damping as defined in ASCE 41-17 as shown in Eq. (1) below. Fig. 6 shows that W3 with inner energy dissipation bars

has less damping due to the reduced elongation of the ED bars compared to W1 and W2 for same drift cycle and unbonded length.

$$\beta_{eff} = \frac{E_d}{2\pi K_{eff}\left(\frac{\Delta_{push}+\Delta_{pull}}{2}\right)^2} \tag{1}$$

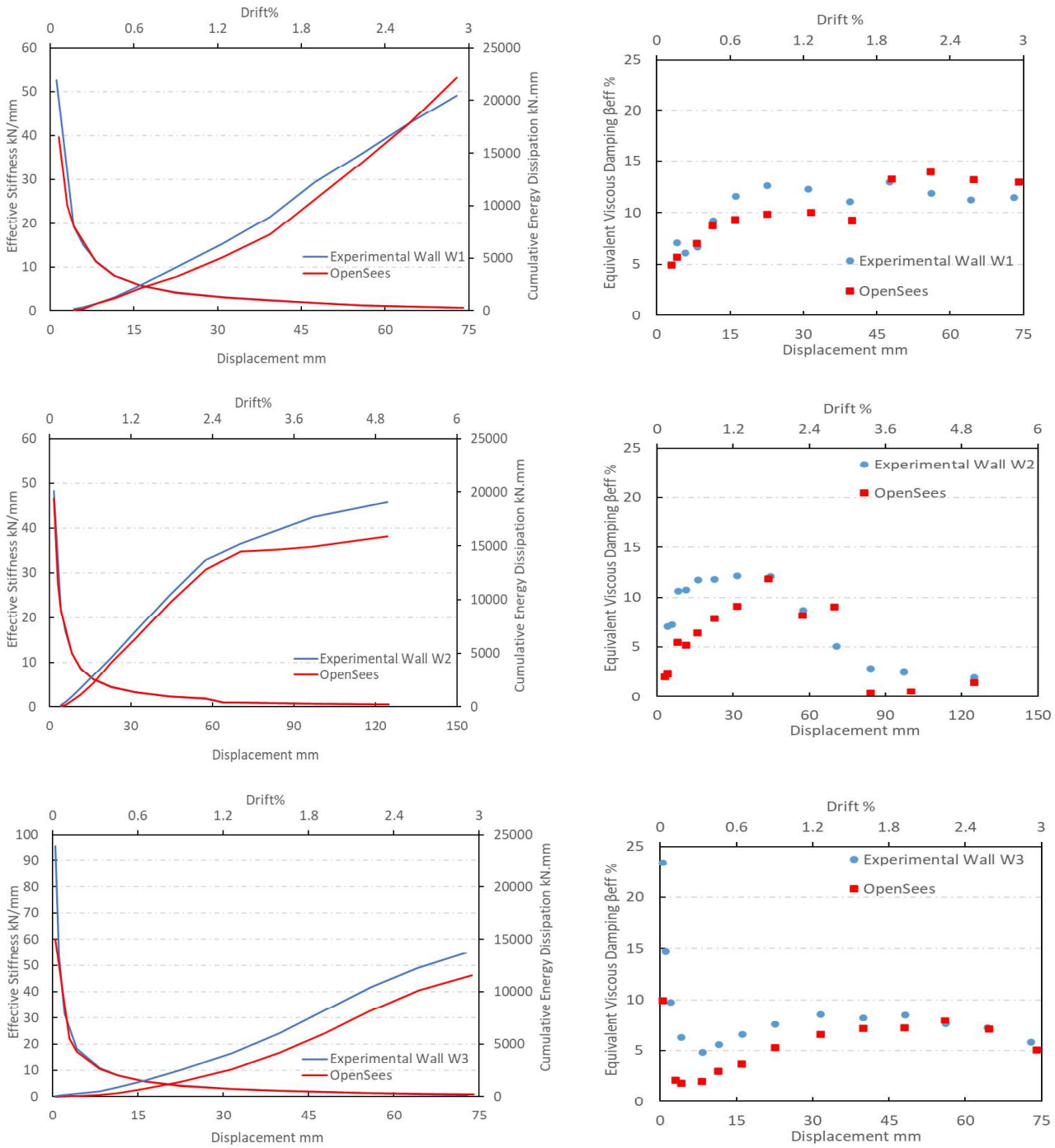

Fig. 6 – Variation of effective stiffness, energy dissipation, and equivalent viscous damping with drift

5. Conclusions

The current study developed a simplified numerical macro-model using OpenSees to simulate the nonlinear behavior of energy dissipation-controlled rocking masonry walls (ED-CRMWs) under cyclic loading. Experimental results of three walls tested by the authors were used to validate the developed model. The validation results demonstrated that the model was able to capture very well the main relevant characteristics of the wall behavior such as force displacement response, lateral load capacity, yield and ultimate displacements, displacement ductility, hysteretic shape and pinching behavior, effective stiffness, and energy dissipation at different drift levels.

The results showed that controlled rocking masonry walls without unbonded post-tensioning tendons can be simulated from a global response perspective using a simplified macro-model that is relatively computationally efficient and that requires only material and geometric properties of the wall, rather than requiring calibration for each experimental result. Research is also underway to use the developed model to investigate the inelastic dynamic behavior of ED-CRMWs under seismic loads.

6. Acknowledgements

The financial support for this project was provided through the Canadian Concrete Masonry Producers Association (CCMPA), the Canada Masonry Design Centre (CMDC), the Natural Sciences and Engineering Research Council (NSERC) and the Ontario Centres of Excellence (OCE).

7. Copyrights

8. References

[1] Priestley M, Sritharan, S, Conley J, Pampanin S (1999): Preliminary results and conclusions from the PRESSS five-story precast concrete test building. *PCI Journal*, **44** (6), 42-67.

[2] Nakaki S, Stanton J, and Sritharan S (1999): An overview of the PRESSS five-story precast concrete test building. *PCI Journal*, **44** (2), 26-39.

[3] Holden T, Restrepo J, Mander J (2003): Seismic performance of precast reinforced and prestressed concrete walls. *Journal of Structural Engineering*, **129** (3), 286-296.

[4] Pérez F, Sause R, Pessiki S (2007): Analytical and experimental lateral load behavior of unbonded posttensioned precast concrete walls. *Journal of Structural Engineering,* **133** (11), 1531-1540.

[5] Laursen P, Ingham J (2004): Structural testing of large-scale posttensioned concrete masonry walls. *Journal of Structural Engineering*, **130** (10), 1497-505.

[6] Hassanli R, ElGawady M, Mills J (2016): Experimental investigation of in-plane cyclic response of unbonded-posttensioned masonry walls. *Journal of Structural Engineering*, **142** (5), 04015171-1-15.

[7] Kalliontzis D, Schultz A (2017): Improved estimation of the reverse-cyclic behavior of fully-grouted masonry shear walls with unbonded post-tensioning. *Eng Struct*, **145**, 83–96.

[8] Yassin A, Ezzeldin M, Steele T, Wiebe L (2020): Seismic Collapse Risk Assessment of Posttensioned Controlled Rocking Masonry Walls. *Journal of Structural Engineering*, **146** (5), 04020060.

[9] FEMA (2012). Next-Generation Methodology for Seismic Performance Assessment of Buildings, FEMA P-58, Washington, D.C

[10] Yassin A, Ezzeldin M, Wiebe L (2021): Experimental Assessment of the Seismic Performance of Controlled Rocking Masonry Walls without Post-Tensioning. *14th Canadian Masonry Symposium*, Montreal, Canada. (Submitted).

[11] McKenna F, Fenves G, Scott M (2000): Open system for earthquake engineering simulation. University of California, Berkeley, CA.

[12] Priestley M, Elder D (1983): Stress-strain curves for unconfined and confined concrete masonry. *ACI Journal*, **80** (19), 192-201.

[13] Pennucci D, Calvi G, Sullivan T (2009): Displacement-based design of precast walls with additional dampers. *Journal of Earthquake Engineering*, **13** (1), 40-65.

[14] Henry R, Brooke N, Sritharan S, Ingham J (2012): Defining concrete compressive strain in unbonded post-tensioned walls. *ACI Journal*, **109** (1), 101-112.

[15] Seismic Evaluation and Retrofit of Existing Buildings, 2017 edition, American Society of Civil Engineers, Reston, Virginia, 2017.

[16] Hose Y, Seible F (1999): Performance evaluation database for concrete bridge components and systems under simulated seismic loads. Technical Report PEER, Pacific Earthquake Engineering Research, Berkeley, USA.

